

# Technical note: Time lag correction of aquatic eddy covariance data measured in the presence of waves

P. Berg<sup>1\*</sup>

C. E. Reimers<sup>2</sup>

J. H. Rosman<sup>3</sup>

M. Huettel<sup>4</sup>

M. L. Delgard<sup>1</sup>

M. A. Reidenbach<sup>1</sup>

T. Özkan-Haller<sup>2</sup>

1) Department of Environmental Sciences, University of Virginia, Charlottesville, Virginia

2) College of Earth, Ocean and Atmospheric Sciences, Oregon State University, Corvallis, Oregon

3) Institute of Marine Sciences, University of North Carolina at Chapel Hill, Morehead City, North Carolina

4) Department of Earth, Ocean and Atmospheric Science, Florida State University, Tallahassee, Florida

\* Corresponding author: E-mail: [pb8n@virginia.edu](mailto:pb8n@virginia.edu)

## Abstract

Extracting benthic oxygen fluxes from eddy covariance time series measured in the presence of surface gravity waves requires careful consideration of the temporal alignment of the vertical velocity and the oxygen concentration. Using a model based on linear wave theory and measured eddy covariance data, we show that a substantial error in fluxes can arise if these two variables are not aligned correctly in time. We refer to this error in flux as the time lag bias. In one example, produced with the wave model, we found that an offset of 0.25 s between the oxygen and the velocity data produced a two-fold overestimation of the flux. In another example, relying on nighttime data measured over a seagrass meadow, a similar offset reversed the flux from an uptake of  $-50 \text{ mmol m}^{-2} \text{ d}^{-1}$  to a release of  $40 \text{ mmol m}^{-2} \text{ d}^{-1}$ . The bias is most acute for data measured at shallow-water sites with short-period waves and low current velocities. At moderate or higher current velocities ( $> 5 - 10 \text{ cm s}^{-1}$ ), the bias is usually insignificant. The widely used traditional time shift correction for data measured in unidirectional flows, where the maximum numerical flux is sought, should not be applied in the presence of waves because it tends to maximize the time lag bias, or give unrealistic flux estimates. Based on wave model predictions and measured data, we propose a new time lag correction that minimizes the time lag bias. The correction requires that the time series of both vertical velocity and oxygen concentration contain a clear periodic wave signal. Because wave motions are often evident in eddy covariance data measured at shallow-water sites, we encourage more work on identifying new time lag corrections.

# 1 Introduction

**1.1 Background** – Eddy covariance (or eddy correlation) measurements of scalar fluxes under water have been performed for many years. The earliest studies focused on measurements of heat fluxes under sea ice (McPhee 1992; Fukuchi et al. 1997; Shirasawa et al. 1997) and salt fluxes in a salt wedge estuary (Partch and Smith 1978). More recently, concurrent heat and salt fluxes have also been measured over marine permeable sandy sediments as tracers for groundwater seepage (Crusius et al. 2008). Over the last 10 years, the aquatic eddy covariance technique has become a widely accepted approach for measuring oxygen fluxes between benthic ecosystems and the overlying water (Berg et al. 2003). In that time, the number of users has grown rapidly, and the technique has been applied under very different field settings such as muddy and sandy sediments (Berg et al. 2003; Kuwae et al. 2006; Glud et al. 2010), deep ocean sediments (Berg et al. 2009) coral reefs (Long et al. 2013; Cathalot et al. 2015; Rovelli et al. 2015), and seagrass meadows (Hume et al. 2011; Rheuban et al. 2014; Long et al. 2015). With a few exceptions, all of the recently published aquatic eddy covariance studies have focused on oxygen fluxes. Oxygen fluxes are also the focus of this study, but its findings apply to all scalar fluxes.

The aquatic eddy covariance technique has advantages over other methods for measuring fluxes between the benthic environment and the overlying water, including its non-invasive nature (Lorrai et al. 2010), high temporal resolution (Rheuban and Berg 2013), and ability to integrate over a large benthic surface (Berg et al. 2007). As a result, the technique is poised for widespread use in aquatic science, analogous to the development in atmospheric boundary layer research where the equivalent approach is now the preferred standard method for measuring land-air fluxes (Baldocchi 2003). As part of the further development of the technique in aquatic environments, a few challenges must be addressed. Procedures for calculating fluxes from raw data must be refined to minimize errors and uncertainties that may be unique to aquatic applications. The procedures used today are largely adapted directly from atmospheric boundary layer research, where the eddy covariance technique has been used for more than six decades (Priestley and Swinbank 1947; Swinbank 1951).

**1.2 Formulation of problem** – This study focuses on estimating oxygen fluxes under a set of field conditions that do not occur in the atmosphere, but are very common under water at shallow-water sites. Here, surface gravity waves can cause oscillatory motion throughout the water column to the benthic surface, and give rise to a unique set of challenges when eddy fluxes are extracted. Some of these challenges are directly linked to limitations of the eddy covariance instrumentation available today. Although fast-responding oxygen sensors are used in eddy covariance measurements, their speed is still limited relative to the velocity sensor (e.g. a Vector Acoustic Doppler Velocimeter (ADV) from Nortek AS). Clark-type oxygen microelectrodes used for eddy covariance typically have response times ( $t_{90\%}$ ) of 0.2 to 0.5 s (Berg et al. 2003; Attard et al. 2015; Donis et al. 2015). Newer optical sensors that have been developed in recent years have comparable or somewhat longer response times of 0.2 to 0.8 s (Chipman et al. 2012; Murniati et al. 2015; Berg et al. in press). This means that the time series of the two key variables from which eddy fluxes are derived, the vertical velocity and oxygen concentration, are never perfectly aligned in time. Also, because the ADV derives its data from acoustic backscatter of suspended particles moving through its  $\sim 2 \text{ cm}^3$  measuring volume, the oxygen sensor must be positioned outside of this volume to avoid disturbing the velocity measurements. Depending on the instantaneous flow direction and magnitude, this physical separation can increase or decrease the time lag between the two time series.

**1.3 Traditional time lag correction** – For measurements in unidirectional flows with thin fast-responding Clark-type microelectrodes ( $t_{90\%} < 0.3 \text{ s}$ ) that can be positioned at the edge of the ADV's measuring volume, the temporal misalignment usually has insignificant effects on the flux estimate (Berg et al. 2013). Inspection of the cumulative co-spectrum between the vertical velocity and the oxygen concentration can confirm or reject this on a case-by-case basis. Specifically, a correction is unnecessary in the absence of a local extremum in the co-spectrum near 1 Hz (Berg et al. 2013). In situations when the misalignment does affect the calculated eddy flux, a straight-forward correction has been adapted from atmospheric boundary layer research, in which the oxygen data are successively shifted in time relative to the velocity data in order to find the maximum numeric flux, or cross-

correlation (Fan et al. 1990; McGinnis et al. 2008; Lorrai et al. 2010). Figure 1 shows an example of this correction applied to data measured in a river with a unidirectional flow of  $\sim 16 \text{ cm s}^{-1}$  and using a new dual oxygen-temperature sensor. This sensor has a 1 cm tip diameter and a response time ( $t_{90\%}$ ) for oxygen of 0.51 s, which was measured by inserting it from air into a water bath (Berg et al. in press). The center of the sensor was positioned  $\sim 2.5 \text{ cm}$  downstream from the center of the ADV's measuring volume.

**1.4 Scope of work** – We will show that even small temporal misalignment between the vertical velocity and the oxygen concentration, inherently imbedded in all present eddy covariance data, can lead to significant errors in the fluxes extracted from data measured in the presence of waves. We refer to this error as the time lag bias, and show that the traditional time lag correction illustrated in Fig. 1 will fail. Using a model based on linear wave theory and measured data, we explain the cause of the bias and examine its potential magnitude. We then propose a new correction for this time lag, which minimizes the time lag bias, and test it on two sets of measured data. We encourage more work on identifying new time lag corrections and provide a link from where all of the raw data used in this study can be downloaded.

## **2 Methods**

**2.1 Illustration of the problem using a wave model** – The two-dimensional model for progressive waves and their effect on the oxygen concentration at a fixed height above the sediment surface is presented in Appendix A. In short, the model, which is based on linear wave theory, describes the horizontal and vertical wave orbital velocities and the variation in oxygen concentration generated by the up-and down movement of the natural oxygen gradient as a function of time as they would be recorded under ideal conditions, without any time lag and at exactly the same location. It is assumed that any local horizontal variations in oxygen uptake or release at the sediment surface has been smeared out by turbulent mixing at this location. Model parameter values (Table A1, Appendix A), including a sediment uptake of  $-368 \text{ mmol m}^{-2} \text{ d}^{-1}$  were adapted or estimated from the eddy covariance data reported by Berg and Huettel (2008) from a shallow-water site

1 exposed to surface waves. The values are well within the range for which linear wave  
2 theory applies. Specifically, ratios of wave amplitude to wavelength and wave amplitude to  
3 water depth should both be  $\ll 1$  (Kundu 1990). Using the equations listed in Appendix A,  
4 gives a wavelength of 7 m, and therefore, ratios of 0.008 and 0.04, respectively. The model  
5 was used to generate theoretical time series of the wave velocity and wave-generated  
6 variation in oxygen concentration that were then shifted in time relative to one another to  
7 illustrate how a time lag can affect the flux calculation.

8 The modeled data were found to mimic the averaged nighttime conditions reported  
9 by Berg and Huettel (2008) well. As illustrated in Fig. 2a, the simulated vertical wave  
10 velocity ( $\tilde{w}$ ) varied between  $\sim \pm 2 \text{ cm s}^{-1}$ , while the associated up-and down movement of  
11 the natural oxygen gradient established by the sediment's uptake produced  $\text{O}_2$   
12 concentration oscillations ( $\tilde{\text{O}}_2$ ) of  $\sim \pm 1 \mu\text{mol L}^{-1}$ . These data are for the case where the  
13 velocity and oxygen concentration are "recorded" without any time lag and at exactly the  
14 same location. Furthermore, the simulated data exclude any current-driven turbulence so  
15 that variations in velocity and concentration are due to wave orbital motion only. The  
16 potential for a significant time lag bias (either positive or negative), which can arise from  
17 the wave signal alone in eddy covariance data, becomes apparent when shifting the oxygen  
18 data stepwise in time relative to the velocity data and recalculating the eddy flux for each  
19 shift (Fig. 2b).

20 The model and its results in Fig. 2 reveal key characteristics of the time lag bias due  
21 to waves:

- 22 1) As soon as there is a time lag between the velocity and the oxygen measurements  
23 (time shift  $\neq 0$ , Fig. 2b), a bias in the flux estimate will arise.
- 24 2) Because oxygen sensors do not have an instant response, and because velocity and  
25 oxygen data are not measured at exactly the same location, fluxes may be biased if  
26 wave-driven fluctuations in velocity and oxygen concentration can be identified.
- 27 3) The size of the time lag bias scales with the mean oxygen concentration gradient in  
28 the water column, therefore, it scales with the real flux.

- 4) The time lag bias can have the opposite sign of the real flux.
- 5) The maximum time lag bias can exceed the real flux.
- 6) For short-period waves, here 2.3 s, a time lag of only 0.20 s can give a bias equal to the real flux.
- 7) The traditional time shift correction, which works well in unidirectional flow (Fig. 1), will tend to identify the time shift associated with the maximum time lag bias.
- 8) The time lag bias can be minimized if the appropriate time shift is applied (Fig. 2b).

The vertical gradient in oxygen concentration is less pronounced for field situations with substantial vertical turbulent mixing. As a result, eddy fluxes calculated from data measured at sites with significant unidirectional currents and rough sediment surfaces, that stimulate vertical mixing (Rattray and Mitsuda 1974; Boudreau and Jorgensen 2001), will be less sensitive to time lag bias, even if orbital wave motions are present. The example in Fig. 2, where the maximum bias was found to be 180% of the real flux, was based on a mean current velocity of  $1.0 \text{ cm s}^{-1}$  and a sediment surface roughness parameter of 2 mm (Table A1). For rougher surfaces, for example with a roughness of 10 mm, additional simulations showed that the maximum bias decreased from 180 to 110% of the real flux. A much larger reduction in maximum bias was seen with increasing current velocity as illustrated in Fig. 3. For example, an increase in velocity from 1 to  $5 \text{ cm s}^{-1}$  or from 1 to  $10 \text{ cm s}^{-1}$  reduced the time lag bias by a factor of 5 and 10, respectively, as the vertical gradient was reduced.

When using the eddy covariance instrumentation available today, there will always be a time lag between the velocity and the oxygen data, and therefore, the sensitivity of the flux calculation to even small time lags, as illustrated in Fig. 2b, can compromise the eddy flux estimated from data measured in the presence of waves.

**2.2 Illustration of new time lag correction using wave model data** – In addition to illustrating the time lag bias, the modeled data in Fig. 2a also point to a new approach for a time lag correction. From  $\tilde{w}$ , the vertical displacement due to wave orbital motion,  $\tilde{z}$ , can be estimated as

$$\tilde{z} = \int \tilde{w} dt \quad (1)$$

This variable, also shown in Fig. 2a, expresses the instantaneous relative elevation of a water parcel that is moved up and down at the vertical wave orbital velocity  $\tilde{w}$ . Defining the positive z-direction upward,  $\tilde{z}$  increases when  $\tilde{w}$  is positive, and vice versa (Fig. 2a). Due to the positive gradient in mean oxygen concentration created by the sediment's consumption of oxygen, a minimum in  $\tilde{O}_2$  will coincide exactly with a maximum in  $\tilde{z}$  in the absence of a time lag, and vice versa (Fig. 2a). Because this combination corresponds to a minimum in cross-correlation (most negative cross-correlation) of  $\tilde{z}$  and  $\tilde{O}_2$ , a new correction for the time lag in measured data can be defined by shifting the  $\tilde{O}_2$  data relative to the  $\tilde{z}$  data until this minimum is located. If instead, the sediment releases oxygen due to benthic photosynthetic production, the mean oxygen concentration gradient is negative and a minimum in  $\tilde{O}_2$  will be matched by a minimum in  $\tilde{z}$ , and vice versa. In this case, the time lag correction can be defined as giving a maximum in cross-correlation of  $\tilde{z}$  and  $\tilde{O}_2$ . As a result of these two different situations, in which the sediment consumes or releases oxygen, a general correction can be defined by locating maxima or minima in the cross-correlation of  $\tilde{z}$  and  $\tilde{O}_2$ . Complications in this correction arise if there is no clear vertical gradient in mean oxygen concentration, for example at dawn and dusk, when oxygen production may match respiration, or in situations where vertical mixing due to substantial current is so vigorous that the vertical oxygen gradient diminishes. These cases are discussed in detail below.

**2.3 Illustration of new time lag correction using measured data** – Figure 4 shows an example of the new correction applied to a 15 min measured eddy covariance data segment, which is the typical time interval used to calculate one eddy flux value (Berg et al. 2003). The data were measured during nighttime over a dense seagrass meadow using a new robust oxygen optode with no stirring sensitivity and a response time ( $t_{90\%}$ ) of 0.51 s when inserted from air into a water bath (Berg et al. in press). The measuring height was 30 cm above the sediment surface, water depth 90 cm, significant wave height 5 cm, wave velocity 2.6 cm s<sup>-1</sup>, and the mean current velocity 0.8 cm s<sup>-1</sup>. To isolate the wave signal from other less dynamic variations in the velocity and oxygen concentration before



calculating the cross-correlation of  $\tilde{z}$  and  $\tilde{O}_2$ , a 385 data point (6.02 s) running average was removed from the raw 64 Hz data. An example of the resulting data is shown in Fig. 4a. The eddy flux itself (Figs. 4b, 4c) was calculated following standard flux calculation procedures based on linear de-trending (Lee et al. 2004; Berg et al. 2009; Attard et al. 2014). Therefore, the estimated eddy flux represents the real flux plus any time lag bias. The 15 s data segment in Fig. 4a shows a distinct wave signal in  $\tilde{z}$  and  $\tilde{O}_2$ , which is a prerequisite for the time lag correction to work. Furthermore, these results, based on measured data, confirm the modeled results shown in Fig. 2, and reveal that the eddy flux (here the real flux plus the time lag bias) can vary substantially and attain both positive and negative values depending on the time shift applied (Fig. 4b). The results underline the notion that obtaining the best estimate of the real flux hinges on a properly determined time shift. In this case, the corrected flux was associated with a time shift of 0.78 s, defined by a distinct minimum in cross-correlation of  $\tilde{z}$  and  $\tilde{O}_2$  (Fig. 4b). This shift should be seen in relation to the sensor's own response time ( $t_{90\%} = 0.51$  s). These values and how they relate are discussed in detail below. The correction reduced the derived flux from -117 to -51 mmol m<sup>-2</sup> d<sup>-1</sup>, or to a value corresponding to 44% of the non-corrected flux (Fig. 4c).

Finally, the data revealed that the traditional time shift correction, where the maximum numerical flux is sought, will lead to substantial overestimation of the flux (Fig. 4b) if negative time shifts are allowed (moving the oxygen data forward in time relative to the velocity data). On the contrary, if negative time shifts are excluded, a positive flux will be predicted (Fig. 4b) which does not make sense for nighttime measurements.

### 3 Results

The new time lag correction was tested on two eddy covariance data sets that were 4 h and 16 h long. Both were measured at shallow-water sites and were characterized by relatively low current velocities and short-period waves, which caused clear wave-driven fluctuations in vertical velocity and oxygen concentration. Consequently, these two data examples had the characteristics expected to produce sizeable time lag biases. In both cases, the wave signal was separated from other less dynamic variations before calculating

the cross-correlation of  $\tilde{z}$  and  $\tilde{O}_2$ . The prior was done by subtracting a running average produced using a filter width of 4 times the wave period from the measured data.

**3.1 Application of new time lag correction, first example** – The first data set (Fig. 5) was measured at dusk over the same dense seagrass meadow and with the same fast-responding oxygen optode (Berg et al. in press) as described in Section 2.3. Again, the measuring height was 30 cm above the sediment.

The 60 s data segment (Fig. 5a) shows, as the previous example (Fig. 4a), a distinct wave signal in  $\tilde{z}$  and  $\tilde{O}_2$  with a  $\sim 1.5$  s period. Wave groups (i.e. sets of 1.5 s waves) with a  $\sim 11$  s period are also visible. The significant wave height averaged 4 cm (Fig. 5b), wave velocity averaged  $2.4 \text{ cm s}^{-1}$ , and the current changed in direction and also in strength between  $0.2$  and  $2.5 \text{ cm s}^{-1}$  with an average of  $1.0 \text{ cm s}^{-1}$ , while the water depth varied between 80 and 140 cm. Unambiguous variations in  $\tilde{z}$  and  $\tilde{O}_2$ , with amplitudes of  $\sim 0.5$  cm and  $\sim 0.5 \mu\text{mol L}^{-1}$ , respectively, allowed precise determination of minima in cross-correlation of  $\tilde{z}$  and  $\tilde{O}_2$  which gave virtually the same time shift for every 15 min time interval used for individual flux estimates (Fig. 5c). The averaged time shift was  $0.85 \pm 0.013 \text{ s}$  (SE,  $n = 16$ ), and the correction reduced the averaged flux from  $-117 \pm 8.9$  to  $-70 \pm 9.7 \text{ mmol m}^{-2} \text{ d}^{-1}$  (SE,  $n = 16$ ), or by a factor of 0.60 (Fig. 5d).

**3.2 Application of new time lag correction, second example** – The 16-h long data set, covering a period from late afternoon into the next day, was measured over a permeable sandy sediment as previously reported by Berg and Huettel (2008). The measuring height was 12 cm above the sediment, and the oxygen concentration was measured with a Clark-type microelectrode. Parameters for the wave model (Figs. 2, 3) were determined from nighttime data from this deployment.

The 60 s data segment shown in Fig. 6a depicts the time when the wave action was at its maximum (Time  $\sim 620$  min). Currents were stronger and waves larger during this deployment, but the segment contains the same clear correlations between the wave driven fluctuation in  $\tilde{z}$  and  $\tilde{O}_2$  as found in the previous examples (Figs. 4a, 5a). The period of the waves was  $\sim 2.3$  s and  $\tilde{z}$  and  $\tilde{O}_2$  had amplitudes of  $\sim 1$  cm and  $\sim 2.5 \mu\text{mol L}^{-1}$ ,

1 respectively. The significant wave height averaged 13 cm (Fig. 6b), wave velocity averaged  
2  $6.2 \text{ cm s}^{-1}$ , and the current velocity changed in direction and also in strength between 0.6  
3 and  $5 \text{ cm s}^{-1}$  (Fig. 6b) with an average of  $2 \text{ cm s}^{-1}$ . In all 67 of the 15 min long time intervals  
4 used for individual flux estimates, an extremum was found in the cross-correlation of  $\tilde{z}$  and  
5  $\tilde{O}_2$ . The optimum time shift corresponded to a minimum correlation for the first part of the  
6 deployment (Time < 1200 min) when the oxygen flux was negative, and a maximum  
7 correlation for the rest of the deployment, consistent with an oxygen release (Fig 6c).  
8 Averaged over the night, the correction reduced the flux from the previously reported  $-368$   
9  $\pm 21$  to  $-182 \pm 11 \text{ mmol m}^{-2} \text{ d}^{-1}$  (SE,  $n = 45$ ), or by a factor of 0.49 (Fig. 6d). This corrected  
10 flux is still almost twice the size of the flux derived from concurrent *in situ* chamber  
11 measurements (Huettel and Gust 1992; Berg and Huettel 2008). The averaged time shift for  
12 the entire deployment was  $1.11 \pm 0.04 \text{ s}$  (SE,  $n = 67$ ).

13 Fluxes shown in Fig. 5 were calculated without a traditional rotation (nullification of  
14 the transverse and vertical mean velocities for each 15 min based flux calculation, Lee et al.  
15 (2004); Lorrai et al. (2010); Lorke et al. (2013)). The current velocities were too small to  
16 produce robust rotation estimates for most of the deployment. However, for the first part  
17 of the deployment, which had current velocities  $>2 \text{ cm s}^{-1}$ , fluxes calculated without and  
18 with rotation equaled  $-70.3 \pm 12.0$  and  $72.1 \pm 11.0 \text{ mmol m}^{-2} \text{ d}^{-1}$  ( $n = 3$ , SE), respectively.  
19 The rotation angle with the vertical direction was  $7^\circ$ . We see the small difference in the flux  
20 of 2% as an indication of marginal effects of so-called wave bias due to sensor tilt (Grant  
21 and Madsen 1986; Trowbridge 1998; Shaw and Trowbridge 2001). The deployment shown  
22 in Fig. 6 had larger current velocities, and the calculation of fluxes included the rotation  
23 described above.

24 The filter width of 4 times the wave period in the running average used to separate  
25 the wave signal from other less dynamic variations before calculating the cross-correlation  
26 of  $\tilde{z}$  and  $\tilde{O}_2$ , was not critical for the outcome of the time lag correction. For example, for the  
27 data shown in Figs. 5 and 6, the corrected average nighttime fluxes varied within  $\pm 4$  and  
28  $\pm 11\%$ , respectively, when the filter width was changed between 2 to 6 times the wave  
29 period.

## 4 Discussion

The results of this study show that oxygen fluxes extracted from eddy covariance data measured at shallow-water sites with short-period waves and low current flows can be affected by a so-called “time lag bias”. The bias arises because of displacement of the natural vertical oxygen gradient by wave orbital motions, combined with temporal misalignments of the oxygen concentration time series relative to the vertical velocity data. This misalignment cannot be entirely avoided with any eddy covariance instrumentation for aquatic scalar flux measurements available today. As a result, time lag bias, documented here using both modeled and measured data, should be considered when eddy covariance data are measured under such field conditions. Time lag corrections that will minimize this bias are possible, and one is presented in this study.

The theoretical example (Fig. 2), produced with a simple model based on linear wave theory (Appendix A) and fitted to measured data reported by Berg and Huettel (2008), illustrates that the time lag bias can be substantial. The modeled data (Fig. 2a), where all variations were due to wave orbital motions, contain no time lag and represent an idealized situation in which velocity and oxygen data were aligned perfectly in time and space. In this case, there is no time lag bias (time shift = 0, Fig. 2b). The data also showed that an imposed time shift of the simulated oxygen data relative to the velocity data of only 0.20 s led to a bias of 100% of the real flux (Fig. 2b), and that the maximum bias, equaling 180%, was found at a time lag of 0.58 s. The model parameters that gave these substantial time lag biases, including an 11 cm surface displacement amplitude of the waves and a current velocity of  $1 \text{ cm s}^{-1}$  (Appendix A), represent common conditions at many near-shore sites. Additional model calculations showed that the maximum bias, relative to the real flux, diminishes rapidly at increasing current velocity due to enhanced turbulent mixing, which reduces the vertical oxygen concentration gradient (Fig. 3, Appendix A). Thus, concern over a substantial time lag bias should only be under relatively low-current flow conditions.

1       The modeled example also shows that if the oxygen concentration and the vertical  
2 velocity are aligned correctly in time, there is no time lag bias (Fig. 2b), which points to the  
3 foundation of the correction proposed in this study. This correction identifies the time shift  
4 that gives a minimum in cross-correlation (most negative cross-correlation) of the wave-  
5 generated fluctuation in oxygen concentration ( $\tilde{O}_2$ ) and the vertical displacement ( $\tilde{z}$ , Eq. 1)  
6 in situations when the benthic system takes up oxygen (Fig. 4b). Opposite to this, where the  
7 system releases oxygen, a maximum in cross-correlation is sought.

8       Essentially, the same correction could be defined by using the cross-correlation  
9 between  $\tilde{O}_2$  and either the fluctuating water pressure or horizontal wave velocity. The  
10 pressure is recorded by standard ADVs at the same sampling frequency as the velocity and  
11 usually at very low noise levels. However, the ADV we are using (a fixed stem Vector from  
12 Nortek AS) measures the pressure at its lower end bell which is located  $\sim 37$  cm above the  
13 ADV's measuring volume where the velocities are measured. As a result, even a small tilt of  
14 the ADV during measurements can introduce a time lag between the cross-correlated  
15 variables and lead to false corrections. Similarly, the horizontal wave velocity is split in two  
16 when recorded as the ADV's two horizontal  $x$  and  $y$  velocities. Thus, a rather complex  
17 rotation is needed to orient the  $x$  component in the direction of the waves (Reimers et al.  
18 2012). In addition, the ADV's  $x$  and  $y$  velocities are associated with substantially higher  
19 noise levels than the vertical  $z$  velocity. For these reasons, we relied on the integrated  
20 vertical wave velocity (Eq. 1) for the new time lag correction.

21       An attractive feature of the correction is its simplicity, but it has limitations too as it  
22 requires that both the measured vertical velocity and the oxygen concentration contain a  
23 clear periodic wave signal. Consequently, at shallow-water sites with photosynthesizing  
24 sediment surfaces, it may fail during periods at dusk and dawn when the oxygen flux  
25 changes from a release to an uptake, or vice versa, reversing the vertical mean oxygen  
26 concentration gradient. Likewise, the correction may also fail, if the wave signal cannot be  
27 clearly identified due to broad-spectrum wave activity.

1           The new correction identifies one single time shift that is applied to the entire time  
2 interval, typically 15 min, for which a flux is calculated (Figs. 4c, 5c, 6c). Although most of  
3 the temporal misalignment of the oxygen data relative to the velocity data is caused by the  
4 oxygen sensor's response time, the physical distance between the ADV's measuring volume  
5 and the oxygen sensors can play a role too. Because the horizontal wave velocity fluctuates  
6 and reverses in direction in each wave cycle, the optimal instantaneous time shift varies  
7 somewhat in time. It is unknown how much the use of one single time shift for each  
8 individual flux calculation affects the correction.

9           A future refinement of a time lag correction would be to include two contributions, a  
10 larger constant one representing the response time of the oxygen sensor, and a smaller  
11 dynamic one accounting for the spatial separation between the velocity and the oxygen  
12 sensor. The latter contribution, which would obtain both positive and negative values,  
13 could easily be determined from known instantaneous horizontal x and y velocities relative  
14 to the position of the two sensors. As an added benefit, this proposed correction would be  
15 more versatile and work in both unidirectional and wave-driven flows.

16           Another possible correction would be to remove the flux contribution associated  
17 with waves in the frequency domain, instead of the time domain used here. This flux  
18 contribution can, for example, be identified fairly easily in the co-spectrum or cumulative  
19 co-spectrum of the vertical velocity and the oxygen concentration, and then be removed.  
20 This, or similar approaches, are already widely used to remove wave contributions to  
21 Reynolds stresses for wave dominated near-bottom flows (Bricker and Monismith 2007).  
22 However, such corrections should be applied with caution here because part of the real  
23 vertical oxygen flux may be facilitated by wave motions, and thus occur at the wave  
24 frequency. Wave motions over rough benthic surfaces can give rise to eddies or water  
25 parcel ejections at wave frequencies, which expand up into the bottom water, well above  
26 the wave boundary layer (Kemp and Simons 1982; Sleath 1987; Reidenbach et al. 2007).

27           The removal of wave contributions to the covariance of vertical and horizontal  
28 velocity components, usually termed wave bias in Reynolds stress calculations, addresses a

1 somewhat similar, yet different problem than that focused on here. Wave bias arises from  
2 an angular misalignment of the ADV relative to the principal axes of the wave-induced  
3 velocity field and is usually caused by a sensor tilt (Grant and Madsen 1986; Trowbridge  
4 1998; Shaw and Trowbridge 2001). Although there is no time lag between the horizontal  
5 and the vertical velocity components, which are measured by the same instrument, this  
6 angular misalignment can cause significant artificial contributions to Reynolds stress  
7 estimates. The time lag bias addressed here is caused by a temporal misalignment between  
8 the velocity and the oxygen concentration measured with two individual sensors.

9         The relatively large time lag bias found in the modeled example (Fig. 2) was also  
10 seen in the measured data example recorded over a dense shallow-water seagrass meadow  
11 (Fig. 4). The data, covering a 15 min time interval, had an inherent time lag between the  
12 measured oxygen concentration and the velocity, and showed a similar high sensitivity to  
13 imposed time shifts (Fig. 4b vs. 2b). For example, time shifts of 0, 0.27, and 0.47 s led to  
14 eddy fluxes, here representing the real flux plus time lag bias, of -117, 0, and 40 mmol m<sup>-2</sup>  
15 d<sup>-1</sup>, respectively, or a change from a clear uptake, to no flux, to a clear release (Fig. 4b). This  
16 rather extreme, but real, example also shows how important it is to identify the  
17 appropriate time shift to minimize the time lag bias. It further illustrates how the  
18 traditional time shift correction, where the maximum numerical flux is sought, would tend  
19 to give the maximum time lag bias if negative time shifts are allowed (Fig. 4b), or an  
20 unrealistic positive flux, i.e. a net release of oxygen, during nighttime.

21         The wave-driven periodic variation in  $\tilde{O}_2$  and  $\tilde{z}$  (Fig. 4a) produced a clear minimum  
22 in cross-correlation of these two variables that could easily be located (Fig. 4b). This  
23 minimum occurred at a time shift of 0.78 s, which gave a corrected flux that was 44% of the  
24 uncorrected flux (Fig. 4c). For reference, the optimal time shift found for the same oxygen  
25 sensor in unidirectional river flow was on average 0.83 s (Berg et al. in press) and 0.88 s in  
26 the example shown here in Fig. 1. The sensor's own response time ( $t_{90\%}$ ) was measured in  
27 lab tests to be 0.51 s, when inserted from air into a water bath. The somewhat slower  
28 response found in the field, where the sensor was permanently under water, was likely  
29 caused by oxygen concentration equilibration through the thin boundary layer flow that

forms over the oxygen sensing foil (Berg et al. in press). Through detailed model calculations, Berg et al. (in press) showed that a sensor with this response time will virtually capture the entire flux signal if a time lag correction is applied. Specifically, the underestimation of the flux was found to be less than 5%, even in challenging situations at shallow-water sites with substantial unidirectional current flow, where small rapid eddies dominated the vertical turbulent mixing.

In both of the two longer-period data examples covering 4 and 16 h (Figs. 5, 6), the new time lag correction led to considerable reductions in the derived eddy flux. In the first example, including 16 individual flux estimates, each based on 15 min time intervals (Fig. 5c), the average corrected flux was 60% of the uncorrected flux (Fig. 5d), and the time shifts were very similar across all time intervals with an average of 0.85 s (Fig. 5c). The fact that fluctuating variations in velocity and oxygen concentration included both longer-period wave groups and short-period waves (Fig. 5a) did not prevent location of optimal time shifts. In the second example, which used data reported earlier by Berg and Huettel (2008) and included 67 individual flux estimates (Fig. 6c), the average corrected nighttime flux was 49% of the uncorrected flux (Fig. 6d). The individual time shifts showed more variation than in the previous example (Fig. 6c) which was likely caused by the more pronounced variations in the two horizontal velocities and significant wave height (Fig. 6B). The relatively large average time shift which had an average of 1.11 s was not expected because Clark-type electrodes used for eddy covariance typically have response times ( $t_{90\%}$ ) between 0.2 to 0.5 s (Berg et al. 2003; Attard et al. 2014; Rovelli et al. 2015). The most likely reason for the large shift is that the electrode tip was damaged or coated with phyto-detritus or marine mucilage near the beginning of the deployment, notably at min ~460 (Fig. 6C), when the time shift doubled from a value well below 1 s. However, it should be noted that the large time shift is not the reason for the substantial reduction in oxygen flux associated with the correction. In the examples given above, much smaller time shifts had similar large effects on the flux (Figs. 2b, 4b). The corrected flux is still roughly twice the size of the flux that was measured with *in situ* chambers deployed concurrently (Fig. 6d). Fundamental differences between the two flux methods, especially when applied to



1 permeable sandy sediments, may explain this disagreement (Glud 2008; Reimers et al.  
2 2012; Berg et al. 2013).

3 One effect of using a slow-responding electrode is that it may not capture the full  
4 amplitude of a short-period wave signal in oxygen concentration, which, in itself, will add  
5 time lag to the recorded periodic wave signal. Specifically, Berg et al. (in press) showed  
6 through modeling that when for example a 0.5 Hz sinusoidal wave signal in oxygen  
7 concentration is measured with a sensor with a response time ( $t_{90\%}$ ) of 0.5 s, a 0.20 s phase  
8 shift, or time lag, is introduced in the recorded data. While this inevitably will add  
9 substantial time lag bias to calculated fluxes unless a time lag correction is applied (Fig. 2,  
10 4), it may not have a large effect on the electrodes ability to capture the fluctuations  
11 associated with current-driven turbulence. Co-spectral analyses of the oxygen  
12 concentration and vertical velocity typically show that only a small fraction of the flux  
13 contribution is associated with frequencies higher than 0.5 Hz. So, even if a sizeable portion  
14 of the flux signal is lost at high frequencies, it may not affect the total flux significantly.

15 The data in Figs. 4 and 5 were measured with a new robust oxygen optode that in  
16 lab tests showed no stirring sensitivity (Berg et al. in press), whereas the data in Fig. 6 were  
17 recorded with a Clark-type microelectrode, a sensor-type that is known to be affected by  
18 the instantaneous water velocity at its tip due to its consumption of oxygen (Gust et al.  
19 1987; Revsbech 1989; Gundersen et al. 1998). Two new studies have focused on how this  
20 stirring sensitivity can affect eddy flux estimates in unidirectional flows (Holtappels et al.  
21 2015) and in wave environments (Reimers et al. accepted). We cannot rule out that the  
22 oxygen measurements shown in Fig. 6 were affected to some extent by the varying wave  
23 velocity. However, typical characteristic patterns of stirring sensitivity in wave  
24 environments as documented by Reimers et al. (accepted) were not seen in these data.  
25 Firstly, stirring sensitivity tends to have an asymmetric dependency on wave velocity,  
26 meaning that oxygen concentration is more affected by the velocity from one direction than  
27 from the other (Holtappels et al. 2015; Reimers et al. accepted). Signs of this characteristic  
28 pattern are easy to identify, but were not seen in our data (Fig. 6a), which contained more  
29 of a sinusoidal variation in oxygen concentration. Secondly, if instead stirring sensitivity

presents itself as a symmetric dependency on wave velocity, which can happen for example if the fluctuating velocity is perpendicular to the sensor, it would appear as a fluctuations in concentration with a frequency double that of the wave frequency. This also was not seen in our data (Fig. 6a).

To examine further if stirring sensitivity affected our flux calculations, we assumed that the microelectrode used to measure the data shown in Fig. 6 had a stirring sensitivity as characterized by Holtappels et al. (2015), using their fitting function and specific fitting parameter values ( $S_{sen} = 0.7\%$ ,  $n = 0.65$ , and  $B = 30$ ). This particular dependency was found when the electrode was pointing into the mean current which represents the orientation that gives the most dramatic stirring sensitivity (Holtappels et al. 2015). We then applied this function to our data assuming this maximum sensitivity for all horizontal velocity directions. For each time point in our data, we calculated the size of the horizontal velocity, from that, the associated stirring sensitivity, and finally, the oxygen concentration as it should have been measured in the absence of stirring sensitivity. Fluxes calculated using the same velocity data and the uncorrected and corrected oxygen concentrations were then compared. The average nighttime flux for the original data was  $-368.0 \pm 20.6 \text{ mmol m}^{-2} \text{ d}^{-1}$  (SE,  $n = 45$ ), whereas the oxygen data with stirring sensitivity removed gave a flux of  $-370.0 \pm 20.5 \text{ mmol m}^{-2} \text{ d}^{-1}$  (SE,  $n = 45$ ), or a difference of 0.6%. The equivalent calculations for the data with the time lag correction applied, gave averaged fluxes of  $-181.6 \pm 11.2$  and  $-182.7 \pm 11.1 \text{ mmol m}^{-2} \text{ d}^{-1}$ , respectively, or as before, a difference of 0.6%. We, therefore, assess that stirring sensitivity did not play a significant role in any of the data presented in this study.

## 5 Summary and recommendations

The results presented here illustrate that substantial time lag biases can arise in flux estimates from eddy covariance data measured in the presence of surface gravity waves. The problem is most acute for data measured at shallow-water sites with short-period waves and low current flows. At moderate or high current velocities ( $> 5$  to  $10 \text{ cm s}^{-1}$ ), the bias usually is insignificant under typical field conditions. In most situations, the problem

can be effectively addressed by applying the appropriate correction. A simple, but helpful, additional flux calculation that will indicate if time lag bias should be of concern, is to impose a small time shift ( $\sim 0.1 - 0.2$  s) on the measured raw data and re-calculate the flux. If a significant change in flux is found, time lag bias should be investigated further. The widely used traditional time shift correction in unidirectional flows, where the maximum numerical flux is sought, tends to amplify the time lag bias, or give unrealistic flux estimates, and should not be applied if clear wave signals are seen in the data. Although the new correction presented here will minimize the time lag bias, one should always strive to measure eddy covariance data using oxygen sensors with minimum time delay and to measure both the velocity and the oxygen concentration as close to the same location as possible. We encourage more work on these issues because wave motion more often than not appears in eddy covariance data measured at shallow-water marine sites.

## **6 Access to data used in this study**

To facilitate more work on eddy flux calculation from data measured in the presence of waves, the data used in this study can be downloaded from:

<http://faculty.virginia.edu/berg/>

## **7 Acknowledgements**

We thank two anonymous reviewers, reviewer Moritz Holtappels, and Associate Editor Jack Middelburg for helpful and constructive comments on the manuscript. We also thank Rachel E. Michaels for editorial assistance on the manuscript. This study was supported by grants from the National Science Foundation (OCE-1061108, OCE-1061218, OCE-1061364, OCE-1334848, and OCE 1334117) and the University of Virginia.

## Appendix A

A model based on linear wave theory for orbital velocities associated with progressive waves and their effect on the oxygen concentration at a given height over the sediment surface was developed and fitted to existing measured eddy covariance data. The model was used to generate theoretical time series of the wave orbital velocity and the corresponding oxygen concentration at the measuring point of an eddy covariance system. These time series were then shifted in time relative to one another to illustrate how a time lag can bias the flux calculation.

The horizontal and vertical wave orbital velocity components,  $\tilde{u}$  and  $\tilde{w}$ , can be expressed as (Dean and Dalrymple 1991)

$$\tilde{u} = a\omega \frac{\cosh(kh)}{\sinh(kH)} \cos(-\omega t) \quad (\text{A1})$$

and

$$\tilde{w} = a\omega \frac{\sinh(kh)}{\sinh(kH)} \sin(-\omega t) \quad (\text{A2})$$

where  $a$  is the wave surface displacement amplitude,  $\omega$  the angular frequency ( $\omega = 2\pi f$ ,  $f$  is the wave frequency in Hz),  $k$  is the angular wavenumber ( $k = 2\pi/\lambda$ ,  $\lambda$  is the wave length),  $h$  is the measuring height above the bottom, and  $H$  is the total water depth.

A value of  $k$  (or  $\lambda$ ) is difficult to assess from measured velocity time series, but can be estimated from the dispersion equation (Dean and Dalrymple 1991) that relates  $k$ ,  $\omega$ , and  $H$  as  $\omega = \sqrt{gk \tanh(kH)}$  where  $g$  is the acceleration due to gravity. Rearranging this equation,  $k$  can be calculated by iteration as

$$k_{j+1} = \frac{\omega^2}{g \tanh(k_j H)} \quad (\text{A3})$$

where  $j$  is the iteration step number.

The relative vertical displacement of a water parcel,  $\tilde{z}$ , can be found by integrating Eq. A2

$$\tilde{z} = \int_0^t \tilde{w} dt = a \frac{\sinh(kh)}{\sinh(kH)} \cos(-\omega t) \quad (\text{A4})$$

Assuming that a vertical gradient in mean oxygen concentration,  $d\bar{O}_2/dz$ , exists near the bottom due to the uptake or release of oxygen by the sediment, the relative concentration fluctuation can be approximated to first order as

$$\tilde{O}_2 \sim \frac{d\bar{O}_2}{dz} (-\tilde{z}) = -a \frac{d\bar{O}_2}{dz} \frac{\sinh(kh)}{\sinh(kH)} \cos(-\omega t) \quad (\text{A5})$$

The vertical gradient can be estimated from Fick's first law of diffusion applied to vertical turbulent mixing as

$$\frac{d\bar{O}_2}{dz} = - \frac{J_{benthic}}{E_z} \quad (\text{A6})$$

where  $J_{benthic}$  is an assumed known benthic flux and  $E_z$  is the turbulent eddy diffusivity. The latter can be estimated by the semi-empirical equation (Businger and Arya 1975)

$$E_z = \kappa u_* h e^{-2h/H} \quad (\text{A7})$$

where  $\kappa$  is von Karman's constant (0.41) and  $u_*$  is the friction velocity. Finally,  $u_*$ , the sediment surface roughness parameter,  $z_0$ , and the current velocity at the measuring height,  $\bar{u}$ , are related by the classic log velocity profile

$$\bar{u} = \frac{u_*}{\kappa} \ln \left( \frac{h}{z_0} \right) \quad (\text{A8})$$

The model was applied to the eddy covariance data reported by Berg and Huettel (2008) for a shallow-water sandy sediments exposed to waves. Model parameter values in Table A1 were found to give good agreement between modeled and measured fluctuations in velocity and oxygen concentration.

1

2

3

4

Water depth, $H$	140 cm
Measuring height, $h$	12 cm
Wave surface displacement amplitude, $a$	11 cm
Wave frequency, $f$	$0.43 \text{ s}^{-1}$
Wavenumber, $k$	$0.0089 \text{ rad cm}^{-1}$
Current velocity, $\bar{u}$	$1 \text{ cm s}^{-1}$
Sediment surface roughness parameter, $z_0$	0.2 cm
Benthic oxygen flux (uptake), $J_{benthic}$	$-368 \text{ mmol m}^{-2} \text{ d}^{-1}$

5

6 Table A1: Wave model parameters used to produce results in Figs. 2 and 3.

7

## Appendix B

The application of the new time lag correction is straightforward and consists of the step-wise calculations outlined below. The input is two parallel time series of the vertical velocity,  $w_i$ , and the oxygen concentration,  $O_{2\ i}$ , each with  $N$  values  $\Delta t$  apart.

Compute:

1)  $z_1 = 0$ . For  $i = 2$  to  $N$ : Calculate  $z_i = z_{i-1} + w_i \Delta t$ .

2) For  $i = 1$  to  $N$ : De-trend  $z_i$  to get the relative vertical displacement due to waves,  $\tilde{z}_i$ , using for example a running average with a filter width of 4 times the wave period.

3) For  $i = 1$  to  $N$ : De-trend  $O_{2\ i}$  the same way to get  $\tilde{O}_{2\ i}$ .

4) Find the minimum or maximum in cross-correlation of  $\tilde{z}_i$  and  $\tilde{O}_{2\ i}$  depending on if the sediment consumes or releases oxygen, respectively.

5) Shift the  $O_{2\ i}$  data (input data) according to (4), and calculate the flux as usual.

## 8 References

- Attard, K. M., G. N. Glud, D. F. McGinnis, and S. Rysgaard. 2014. Seasonal rates of benthic primary production in a Greenland fjord measured by aquatic eddy correlation. *Limnol. Oceanogr.* **59**: 1555-1569.
- Attard, K. M., H. Stahl, N. A. Kamenos, G. Turner, H. L. Burdett, and R. N. Glud. 2015. Benthic oxygen exchange in a live coralline algal bed and an adjacent sandy habitat: an eddy covariance study. *Marine Ecology Progress Series*???: doi: 10.3354/meps11413.
- Baldocchi, D. D. 2003. Assessing the eddy covariance technique for evaluating carbon dioxide exchange rates of ecosystems: past, present and future. *Global Change Biology* **9**: 479-492.
- Berg, P., R. N. Glud, A. Hume, H. Stahl, K. Oguri, V. Meyer, and H. Kitazato. 2009. Eddy correlation measurements of oxygen uptake in deep ocean sediments. *Limnol. Oceanogr.: Methods* **7**: 576-584.
- Berg, P., and M. Huettel. 2008. Monitoring the seafloor using the noninvasive eddy correlation technique: Integrated benthic exchange dynamics. *Oceanography* **21**: 164-167.
- Berg, P., D. Koopmans, M. Huettel, H. Li, K. Mori, and A. Wüest. in press. A new robust dual oxygen-temperature sensor for aquatic eddy covariance measurements. *Limnol. Oceanogr.: Methods*.
- Berg, P., M. H. Long, M. Huettel, J. E. Rheuban, K. J. McGlathery, R. W. Howarth, K. H. Foreman, A. E. Giblin, and R. Marino. 2013. Eddy correlation measurements of oxygen fluxes in permeable sediments exposed to varying current flow and light. *Limnol. Oceanogr.* **58**: 1329-1343.
- Berg, P., H. Roy, F. Janssen, V. Meyer, B. B. Jorgensen, M. Huettel, and D. de Beer. 2003. Oxygen uptake by aquatic sediments measured with a novel non-invasive eddy-correlation technique. *Marine Ecology Progress Series* **261**: 75-83.
- Berg, P., H. Roy, and P. L. Wiberg. 2007. Eddy correlation flux measurements: The sediment surface area that contributes to the flux. *Limnol. Oceanogr.* **52**: 1672-1684.
- Boudreau, B. P., and B. B. Jorgensen. 2001. *The benthic boundary layer: Transport processes and biogeochemistry*. Oxford University Press, Oxford UK.
- Bricker, J. D., and S. G. Monismith. 2007. Spectral wave-turbulence decomposition. *Journal of Atmospheric and Oceanic Technology* **24**: 1479-1487.
- Businger, J. A., and S. Arya. 1975. Height of the mixed layer in the stably stratified planetary boundary layer. *Advances in geophysics* **18**: 73-92.
- Cathalot, C., D. Van Oevelen, T. Cox, T. Kutti, M. Lavaleye, G. Duineveld, and F. J. R. Meysman. 2015. Cold-water coral reefs and adjacent sponge grounds: Hotspots of benthic respiration and organic carbon cycling in the deep sea. *Frontiers in Marine Science* **2**:37: doi: 10.3389/fmars.2015.00037.
- Chipman, L., M. Huettel, P. Berg, V. Meyer, I. Klimant, R. N. Glud, and F. Wenzhoefer. 2012. Oxygen optodes as fast sensors for eddy correlation measurements in aquatic systems. *Limnology and Oceanography: Methods*.
- Crusius, J., P. Berg, D. J. Koopmans, and L. Erban. 2008. Eddy correlation measurements of submarine groundwater discharge. *Marine Chemistry* **109**: 77-85.
- Dean, R. G., and R. A. Dalrymple. 1991. *Water Wave Mechanics for Engineers and Scientists*. World Scientific, Singapore.



- Donis, D., M. Holtappels, C. Noss, C. Cathalot, K. Hancke, P. Polsenaere, F. Wenzhöfer, A. Lorke, F. J. R. Meysman, and R. N. Glud. 2015. An assessment of the precision and confidence of aquatic eddy correlation measurements. *Journal of Atmospheric and Oceanic Technology* **32**: 642-655.
- Fan, S. M., S. C. Wofsy, P. S. Bakwin, D. J. Jacob, and D. R. Fitzjarrald. 1990. Atmosphere-biosphere exchange of CO<sub>2</sub> and O<sub>3</sub> in the central Amazon forest. *Journal of Geophysical Research: Atmospheres* **95**: 16851-16864.
- Fukuchi, M., L. Legendre, and T. Hoshiai. 1997. The Canada–Japan SARES project on the first-year ice of Saroma-ko Lagoon (northern Hokkaido Japan) and Resolute Passage (Canada High Arctic). *Journal of Marine Systems* **11**: 1-8.
- Glud, R. N. 2008. Oxygen dynamics of marine sediments. *Marine Biology Research* **4**: 243-289.
- Glud, R. N., P. Berg, A. Hume, P. Batty, M. E. Blicher, K. Lennert, and S. Rysgaard. 2010. Benthic O<sub>2</sub> exchange across hard-bottom substrates quantified by eddy correlation in a sub-Arctic fjord. *Marine Ecology Progress Series* **417**: 1-12.
- Grant, W. D., and O. S. Madsen. 1986. The continental shelf bottom boundary layer. *Annu. Rev. Fluid Mech.* **18**: 265 - 306.
- Gundersen, J. K., N. B. Ramsing, and R. N. Glud. 1998. Predicting the signal of O<sub>2</sub> microsensors from physical dimensions, temperature, salinity, and O<sub>2</sub> concentration. *Limnology & Oceanography* **43**: 1932-1937.
- Gust, G., K. Booi, W. Helder, and B. Sundby. 1987. On the velocity sensitivity (stirring effect) of polarographic oxygen microelectrodes. *Neth. J. Sea. Res.* **21**: 255-263.
- Holtappels, M., C. Noss, K. Hancke, C. Cathalot, D. McGinnis, A. Lorke, and R. N. Glud. 2015. Aquatic Eddy correlation: Quantifying the artificial flux caused by stirring sensitive O<sub>2</sub> sensors. *Plos One*.
- Huettel, M., and G. Gust. 1992. Solute release mechanisms from confined sediment cores in stirred benthic chambers and flume flows. *Marine Ecology Progress Series* **82**: 187-197.
- Hume, A. C., P. Berg, and K. J. McGlathery. 2011. Dissolved oxygen fluxes and ecosystem metabolism in an eelgrass (*Zostera marina*) meadow measured with the eddy correlation technique. *Limnol. Oceanogr.* **56**: 86-96.
- Kemp, P. H., and R. R. Simons. 1982. The interaction between waves and a turbulent current: waves propagating with the current. *Journal of Fluid Mechanics* **116**: 227-250.
- Kundu, P. K. 1990. *Fluid Mechanics*, 638 pp. Academic Press, San Diego, California.
- Kuwae, T., K. Kamio, T. Inoue, E. Miyoshi, and Y. Uchiyama. 2006. Oxygen exchange flux between sediment and water in an intertidal sandflat, measured in situ by the eddy-correlation method. *Marine Ecology Progress Series* **307**: 59-68.
- Lee, X., W. Massman, and B. Law. 2004. *Handbook of micrometeorology: A guide for surface flux measurement and analysis*. Kluwer Academic Publishers.
- Long, M. H., P. Berg, D. de Beer, and J. C. Zieman. 2013. In Situ Coral Reef Oxygen Metabolism: An Eddy Correlation Study. *Plos One* **8**: e58581.
- Long, M. H., P. Berg, K. M. McGlathery, and J. C. Zieman. 2015. Sub-Tropical Seagrass Ecosystem Metabolism Measured by Eddy Correlation. *Marine Ecology Progress Series* **529**: 75–90.
- Lorke, A., D. F. McGinnis, and A. Maeck. 2013. Eddy-correlation measurements of benthic fluxes under complex flow conditions: Effects of coordinate transformations and averaging time scales. *Limnology and Oceanography: Methods* **11**: 425 - 437.

- 1 Lorrai, C., D. F. McGinnis, P. Berg, A. Brand, and A. Wüest. 2010. Application of oxygen eddy  
2 correlation in aquatic systems. *Journal of Atmospheric and Oceanic Technology* **27**:  
3 1533-1546.
- 4 McGinnis, D. F., P. Berg, A. Brand, C. Lorrai, T. J. Edmonds, and A. Wuest. 2008.  
5 Measurements of eddy correlation oxygen fluxes in shallow freshwaters: Towards routine  
6 applications and analysis. *Geophysical Research Letters* **35**: 1-5.
- 7 McPhee, M. G. 1992. Turbulent heat flux in the upper ocean under sea ice. *Journal of*  
8 *Geophysical Research* **97**: 5365–5379.
- 9 Murniati, E., S. Geissler, and A. Lorke. 2015. Short-term and seasonal variability of oxygen  
10 fluxes at the sediment–water interface in a riverine lake. *Aquatic Sciences* **77**: 183 -196.
- 11 Partch, E. N., and J. D. Smith. 1978. Time dependent mixing in a salt wedge estuary. *Estuarine*  
12 *and Coastal Marine Science* **6**: 3-19.
- 13 Priestley, C., and W. Swinbank. 1947. Vertical transport of heat by turbulence in the atmosphere,  
14 p. 543-561. *Proceedings of the Royal Society of London A: Mathematical, Physical and*  
15 *Engineering Sciences*. The Royal Society.
- 16 Rattray, M., and E. Mitsuda. 1974. Theoretical analysis of conditions in a salt wedge. *Estuarine*  
17 *and Coastal Marine Science* **2**: 375-394.
- 18 Reidenbach, M. A., J. R. Koseff, and S. G. Monismith. 2007. Laboratory experiments of fine-  
19 scale mixing and mass transport within a coral canopy. *Physics of Fluids* **19**: 075107,  
20 doi:075110.071063/075101.2752189.
- 21 Reimers, C. E., T. Özkan-Haller, A. Albright, and P. Berg. accepted. Microelectrode velocity  
22 effects and aquatic eddy covariance measurements under waves. *Journal of Atmospheric*  
23 *and Oceanic Technology*.
- 24 Reimers, C. E., T. Özkan-Haller, P. Berg, A. Devol, K. McCann-Grosvenor, and R. D. Sanders.  
25 2012. Benthic oxygen consumption rates during hypoxic conditions on the Oregon  
26 continental shelf: Evaluation of the eddy correlation method. *J. Geophys. Res.* **117**: 1-18.
- 27 Revsbech, N. P. 1989. An oxygen microsensor with a guard cathode. *Limnol. Oceanogr.* **34**:  
28 474-478.
- 29 Rheuban, J. E., and P. Berg. 2013. The effects of spatial and temporal variability at the sediment  
30 surface on aquatic eddy correlation flux measurements. *Limnology And Oceanography*:  
31 *Methods* **11**: 351–359.
- 32 Rheuban, J. E., P. Berg, and K. J. McGlathery. 2014. Multiple timescale processes drive  
33 ecosystem metabolism in eelgrass (*Zostera marina*) meadows. *Marine Ecology Progress*  
34 *Series* **507**: 1–13.
- 35 Rovelli, L., K. M. Attard, L. D. Bryant, S. Flögel, H. J. Stahl, M. Roberts, P. Linke, and R. N.  
36 Glud. 2015. Benthic O<sub>2</sub> uptake of two cold-water coral communities estimated with the  
37 non-invasive eddy-correlation technique. *Marine Ecology Progress Series* **525**: 97-104.
- 38 Shaw, W. J., and J. H. Trowbridge. 2001. The Direct Estimation of Near-Bottom Turbulent  
39 Fluxes in the Presence of Energetic Wave Motions. *Journal of Atmospheric and Oceanic*  
40 *Technology* **18**: 1540-1557.
- 41 Shirasawa, K., R. G. Ingram, and E. J. J. Hudier. 1997. Oceanic heat fluxes under thin sea ice in  
42 Saroma-ko Lagoon, Hokkaido Japan. *Journal of Marine Systems* **11**: 9-19.
- 43 Sleath, J. 1987. Turbulent oscillatory flow over rough beds. *Journal of Fluid Mechanics* **182**:  
44 369-409.

- 1 Swinbank, W. C. 1951. The measurement of vertical transfer of heat and water vapor by eddies  
2 in the lower atmosphere. *Journal of Meteorology* **8**: 115-145.
- 3 Trowbridge, J. 1998. On a technique for measurement of turbulent shear stress in the presence of  
4 surface waves. *Journal of Atmospheric and Oceanic Technology* **15**: 290-298.

5

6

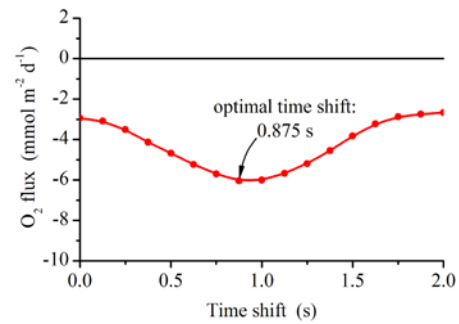
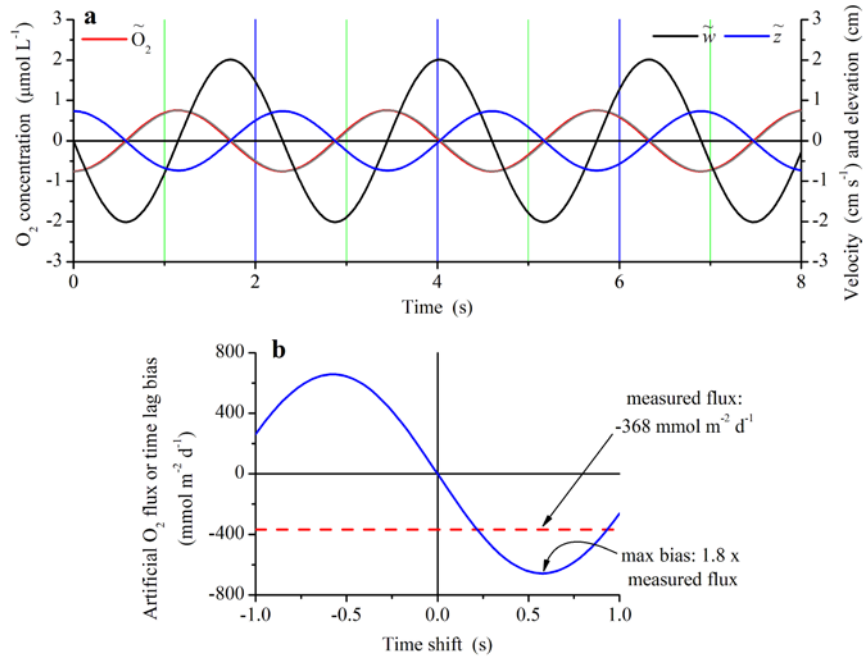
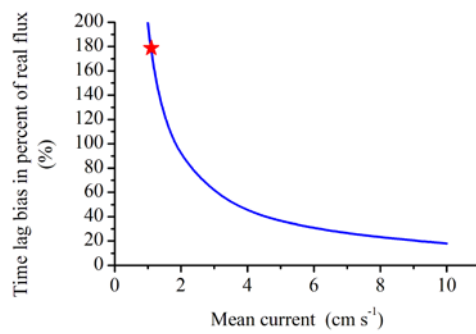


Fig. 1: Example of traditional time lag correction of 8 Hz eddy covariance data measured with a dual oxygen-temperature sensor in unidirectional river flow. The oxygen data are moved back in time relative to the velocity data. The 'best' flux estimate is defined as the maximum numeric flux value and corresponds to an optimal time shift of 0.875 s.



**Fig. 2:** Illustration, using modeled data, of the substantial error, or time lag bias, that can arise in eddy flux estimates from data measured in the presence of waves. Parameters for the model were taken from Berg and Huettel (2008). **(a)** Fluctuations due to wave motion only in vertical velocity ( $\tilde{w}$ ), oxygen concentration ( $\tilde{O}_2$ ), and vertical displacement, ( $\tilde{z}$ , see its definition and use in the text). **(b)** Time lag bias (blue line) at different imposed time shifts, relative to the assumed real flux (red line) which was used to parameterize the model. Positive time shifts move the oxygen data back in time relative to the velocity data.



**Fig. 3:** Reduction in maximum bias with increasing current velocity. The star represents the modeled data shown in Fig. 2b where the maximum bias is 180% of the assumed real flux. Except for the current velocity, and derived friction velocity and turbulent eddy diffusivity (see Appendix A), all other model parameters were kept constant.

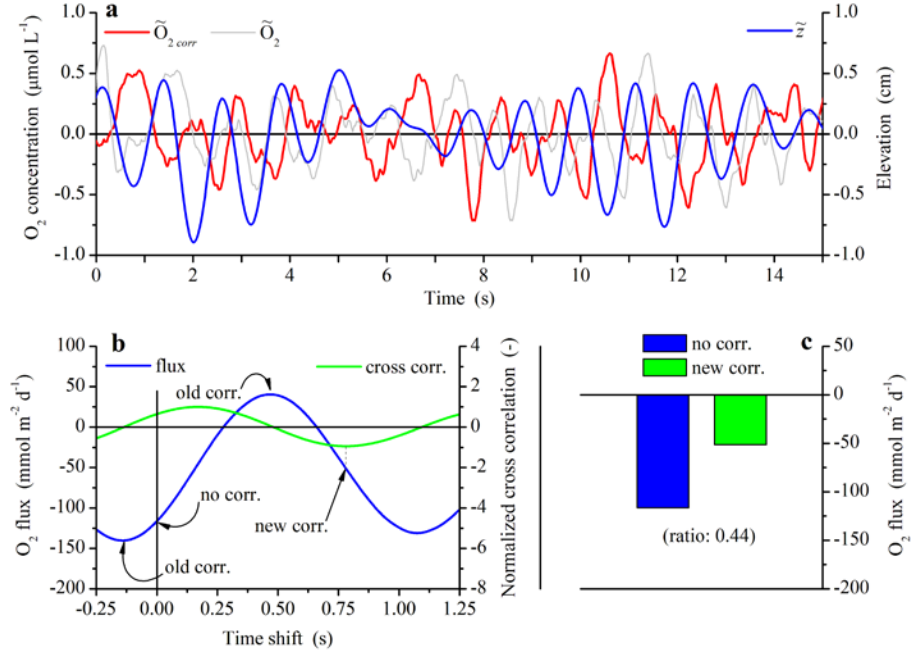


**Fig. 4:** Illustration of the new time lag correction for a 15 min long data segment measured during nighttime over a dense seagrass meadow. **(a)** Fifteen s data segment of the larger 15 min segment showing oxygen concentration fluctuations due to wave motions before ( $\tilde{O}_2$ ) and after the time lag correction ( $\tilde{O}_{2\text{corr}}$ ), and vertical displacement ( $\tilde{z}$ ) calculated from Eq. 1. The 64 Hz data were smoothed by a 17 point (0.27 s) running average to better illustrate the wave signal. **(b)** Eddy flux calculated for the 15 min period for different time shifts and the associated cross-correlation of  $\tilde{z}$  and  $\tilde{O}_2$ . Positive time shifts move the oxygen data back in time relative to the velocity data. **(c)** Oxygen flux calculated without time shift correction and with the new time lag correction (new corr.). The latter was defined as the shift that gave a minimum in cross-correlation of  $\tilde{z}$  and  $\tilde{O}_2$  as illustrated in **b**.

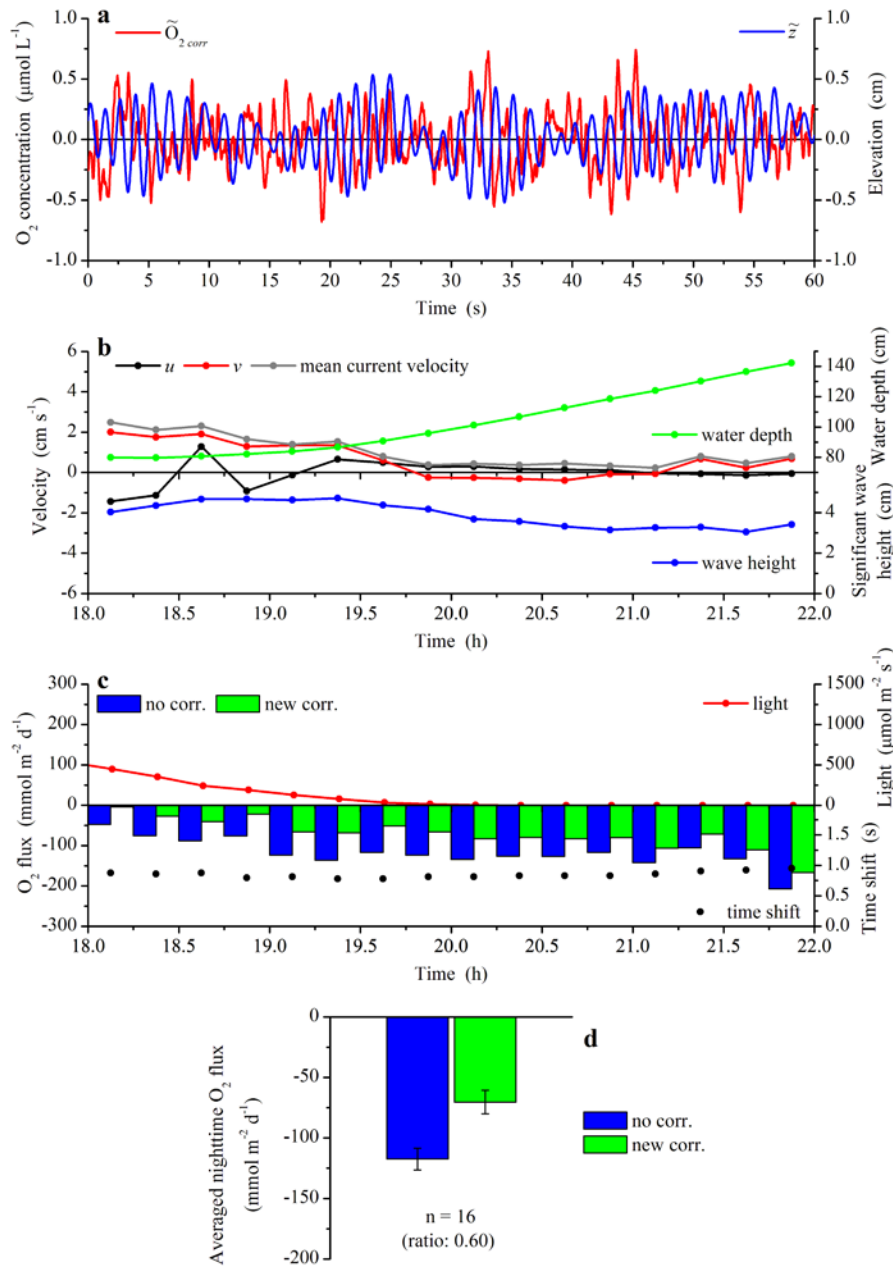


**Fig. 5:** Application of the new time lag correction applied to a 4-h long data segment measured over a dense seagrass meadow. **(a)** Sixty s segment of wave-driven variation in oxygen concentration after correction ( $\tilde{O}_{2,corr}$ ) and vertical displacement ( $\tilde{z}$ ) as calculated from Eq. 1. The 64 Hz data were smoothed by a 17 point (0.27 s) running average to better illustrate the wave signal. **(b)** Fifteen min averages of the two horizontal velocity components ( $u$  and  $v$ ), mean current velocity, water depth, and significant wave height. **(c)** Oxygen flux, one per 15 min, determined without and with the new correction, light (PAR) measured above the seagrass canopy, and the time shift. **(d)** Average flux for nighttime (Time > 18.25 h) before and after correction.



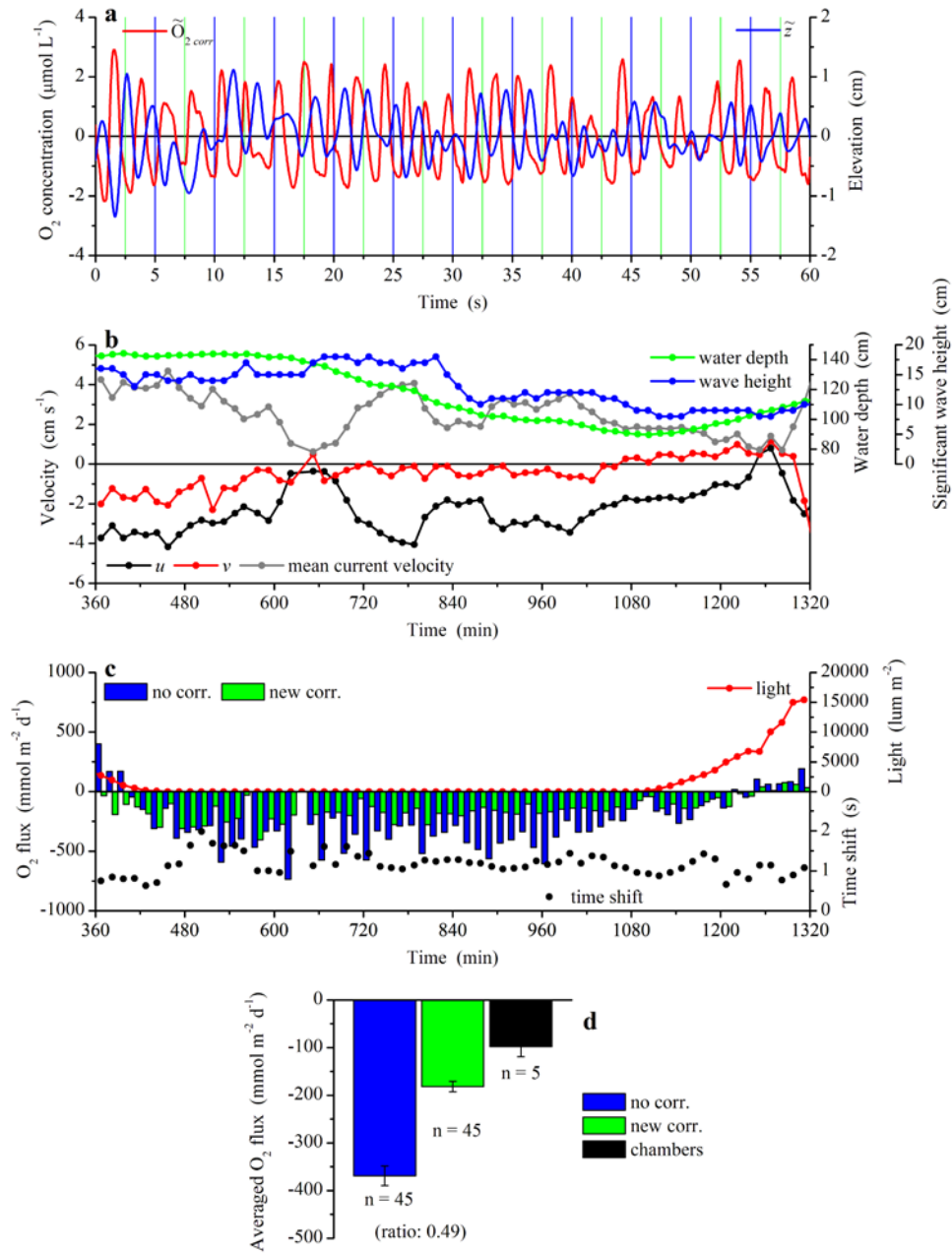


**Fig. 6:** Application of the new time lag correction applied to a 16-h long data segment measured over a permeable sandy sediment and reported earlier by Berg and Huettel (2008). **(a)** Sixty s segment of wave-driven variation in oxygen concentration after correction ( $\tilde{O}_{2\text{corr}}$ ) and vertical displacement ( $\tilde{z}$ ) as calculated from Eq. 1. The data are from when the wave action was at its maximum (Time  $\sim 620$  min). The 64 Hz data were smoothed by a 17 point (0.27 s) running average to better illustrate the wave signal. **(b)** Fifteen min averages of the two horizontal velocity components ( $u$  and  $v$ ), mean current velocity, water depth, and significant wave height. **(c)** Oxygen flux, one per 15 min, determined without and with the new correction, light measured above the sand, and the time shift. **(d)** Average flux for nighttime (450 min  $<$  Time  $<$  1095 min) before and after correction and measured concurrently with *in situ* chambers.